ment (in the mean-square amplitude) of a factor of 4 in the first *two* monolayers of the surface (Fig. 2). Enhanced surface vibrations can have some effect on the quantitative interpretation of the data but clearly will not alter the main conclusion of this study, namely that the major reconstruction of the Si(111)-(7×7) surface involves substantial vertical displacements in two monolayers.

The interpretation of our experiments does not require a presumed model; general features of the surface structure are determined. While these results alone cannot explain the surface periodicity, any realistic model of the 7×7 structure[7] must incorporate the geometric features found here. The ⟨001⟩ data indicate that two layers have large displacements (~0.4 Å) normal to the surface. It is clear that this rules out any model with atoms in bulklike positions, such as a *pure* vacancy model.[8] Partial agreement is obtained with models having only perpendicular displacements, such as the rippled-surface model of Mark, Levine, and McFarlane,[9] which has a relaxation in the first two layers modulated by a small-amplitude ripple. The buckled-surface model of Chadi[10] contains both small parallel displacements and large perpendicular displacements in several layers. This type of model gives the best agreement with the present ion-scattering results. The epitaxial misfit strain model of Phillips[11] also involves lateral and normal displacements.

In conclusion, we have measured the SP intensity in the ⟨111⟩ and ⟨001⟩ directions for the Si(111)-(7×7) surface. The energy dependence of the ⟨111⟩ SP intensity is close to that expected for a bulklike structure and implies that transverse displacements are confined to one to two monolayers with a magnitude of $\lesssim 0.15$ Å. The angular dependence of the ⟨001⟩ SP intensity at 500 keV indicates that two monolayers have displacements of ~0.4 Å perpendicular to the surface. This provides the first definitive evidence that the major reconstruction in Si(111)-(7×7) involves large perpendicular displacements.

[1]L. C. Feldman, P. J. Silverman, and I. Stensgaard, Nucl. Instrum. Methods 168, 589 (1980).
[2]I. Stensgaard, L. C. Feldman, and P. J. Silverman, Surf. Sci. 77, 513 (1978).
[3]J. L'Ecuyer, J. A. Davis, and N. Matsunami, Nucl. Instrum. Methods 160, 337 (1979).
[4]O. H. Nielsen, Institute of Physics, University of Aarhus, Denmark, Internal Report, 1979 (unpublished).
[5]E. Bogh and I. Stensgaard, Phys. Lett. 65A, 357 (1978).
[6]W. Mönch, Surf. Sci. 86, 672 (1979).
[7]For recent reviews, see Ref. 6, and D. E. Eastman, J. Vac. Sci. Technol. 17, 492 (1980).
[8]J. J. Lander and J. Morrison, J. Appl. Phys. 34, 1403 (1963).
[9]P. Mark, J. D. Levine, and S. H. McFarlane, Phys. Rev. Lett. 38, 1408 (1977).
[10]D. J. Chadi, R. S. Bauer, R. H. Williams, G. V. Hansson, R. Z. Bachrach, J. C. Mikkelsen, Jr., F. Houzay, G. M. Guichar, R. Pinchauz, and Y. Petroff, Phys. Rev. Lett. 44, 799 (1980).
[11]J. C. Phillips, Phys. Rev. Lett. 45, 905 (1980).

Diffuse-X-Ray-Scattering Study of the Fast-Ion Conductor β-Ag_2S

R. J. Cava and D. B. McWhan
Bell Laboratoires, Murray Hill, New Jersey 07974
(Received 20 August 1980)

Disks of diffuse scattering are observed at $\vec{q} = \langle \sim 0.6, 0, 0 \rangle$ around the bcc Bragg reflections implying correlations of the Ag ions in the [100] directions. The average correlation length and the inverse Haven's ratio both decrease with increasing temperature. The x-ray measurements provide structural evidence for strongly correlated ionic transport in β-Ag_2S.

PACS numbers: 66.30.Hs, 61.10.-i, 61.55.Hg

The mechanism for the high ionic conductivity in silver-based salts such as α-AgI is currently under active study.[1] The silver ions are highly disordered and can be treated as a "liquid" confined to the channels of the body-centered cubic lattice formed by the iodine ions. In β-Ag_2S, twice as many Ag ions are distributed in the channels of the bcc lattice of sulfur anions, and a caterpillar mechanism[2] for cooperative ionic charge transport has been proposed to explain the anomalously small ratio (Haven's ratio) of the diffusion coefficients derived from tracer and ionic

conductivity measurements.[3,4] In this Letter we present x-ray scattering measurements as a function of temperature which provide structural evidence for a more complex correlated ion motion.

Ag_2S has a first-order phase transition on cooling at 450 K from the cubic electrolyte phase to a monoclinic phase[5] which involves an ordering of the silver ions and a distortion of the sulfur array. The reciprocal lattice of the monoclinic phase is obtained from that of the cubic phase by the transformation

$$\begin{pmatrix} a^* \\ b^* \\ c^* \end{pmatrix} = \begin{pmatrix} 1 & -1 & 0 \\ \frac{1}{2} & \frac{1}{2} & 0 \\ \frac{1}{4} & -\frac{1}{4} & \frac{1}{2} \end{pmatrix} \begin{pmatrix} a_1^* \\ a_2^* \\ a_3^* \end{pmatrix}.$$

The silver ions are distributed over the tetrahedral sites, which are arranged at the vertices of a cubo-octahedron, and over the octahedral sites, which are at the center of the square faces of the cubo-octahedron. Detailed neutron and x-ray studies show the distribution of the Ag ions between the tetrahedral and octahedral sites increases from 2:2 in the monoclinic phase to 3.2:0.8 at a temperature 9° above the transition and to 4:0 at temperatures ~50° above the transition.[5,6] At all temperatures on the cubic phase, the cation density is delocalized in bands along ⟨100⟩ as a result of positional disorder and large anharmonic thermal motion.

The crystals of Ag_2S used in the present study of the diffuse scattering were fragments of a crystal grown by Ohachi and co-workers at 823 K in the stability field of the cubic phase but which had twinned on cooling through the cubic to monoclinic phase transition.[7] The crystals were from the same large crystal employed in the single-crystal neutron-diffraction study.[6] Measurements were made using a high-brilliance Rigaku rotating-anode x-ray generator. The crystal was heated in air, and the temperature was regulated to ~0.2 deg by a Lake Shore temperature controller in conjunction with a thermistor. The diffuse x-ray scattering was studied with monochromatic Mo $K\alpha$ radiation from 435 to 525 K using the fixed-crystal fixed-film technique and was surveyed extensively at 458 K. Quantitative measurements were made from 350 to 568 K with use of a three-crystal diffractometer equipped with a quarter-circle Eulerian cradle. Copper $K\alpha$ radiation was used with a vertically bent pyrolytic-graphite monochromator and a flat graphite analyzer.

The film data showed that in the cubic phase

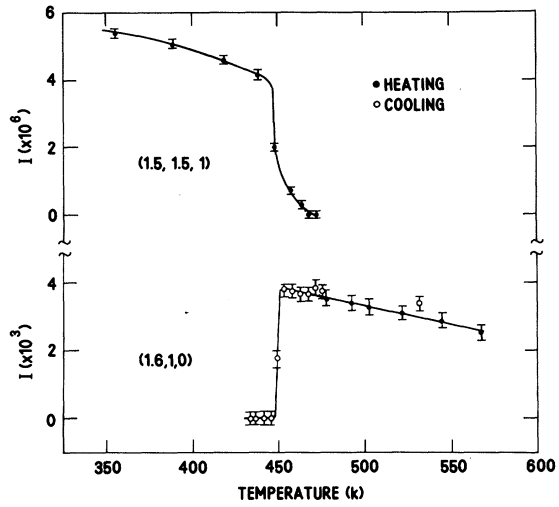

FIG. 1. Intensity of the strongest superlattice peak in the monoclinic phase of Ag_2S (top curve) and of the strongest diffuse disk (bottom curve) vs temperature.

most of the diffuse scattering occurs in the form of disks around the Bragg reflections of the bcc structure at incommensurate q vectors of (0.6, 0, 0) with the strongest scattering at (1.6, 1, 0). Just above the phase transition diffuse scattering was observed at the positions of the strongest Bragg reflections of the low-temperature monoclinic structure [for example, at $(\frac{3}{2}, \frac{3}{2}, 1)$], but this intensity decreased with increasing temperature and was not visible above background by a temperature of ~50 K above the transition. This correlates with the average structure refinements which indicate that the octahedral sites become destabilized as equilibrium silver positions in this temperature region. Diffractometer measurements of the peak intensity versus temperature of the strongest superlattice reflection of the monoclinic phase and of the strongest diffuse disk are shown in Fig. 1. No cooling data are shown for the $(\frac{3}{2}, \frac{3}{2}, 1)$ reflection because of twin formation at the transition.[5] It is clear that the local ordering of the Ag ions in the low- and high-temperature phases are unrelated.

The average size of the correlated regions was determined assuming a model of small domains which diffract incoherently. The correlation lengths parallel, $\xi_{\parallel}$, and perpendicular, $\xi_{\perp}$, to the $\vec{a}$ axis are plotted versus temperature in Fig. 2, and they were determined from the full width at half maximum of the peaks observed in scans taken in the three cubic directions through the disk at (1.6, 1, 0). The variation of the position

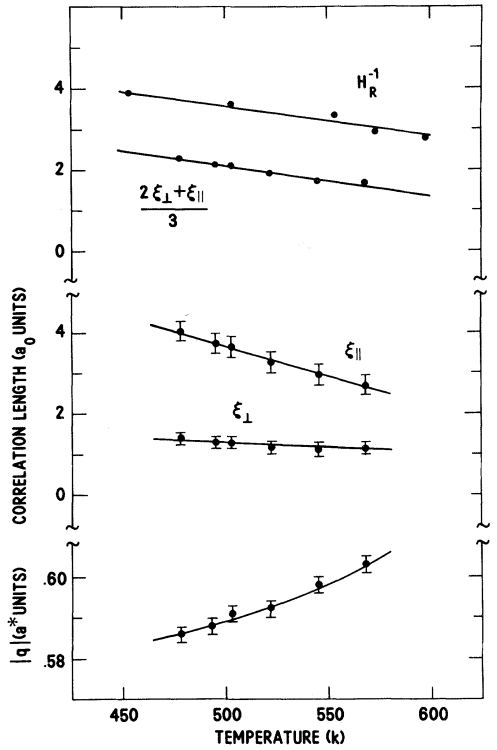

FIG. 2. Variation with temperature of the inverse Haven's ratio (Refs. 3 and 4), the average correlation length, the correlation lengths ∥ and ⊥ to [100], and the position of the disk of diffuse scattering at $(1+q, 1, 0)$.

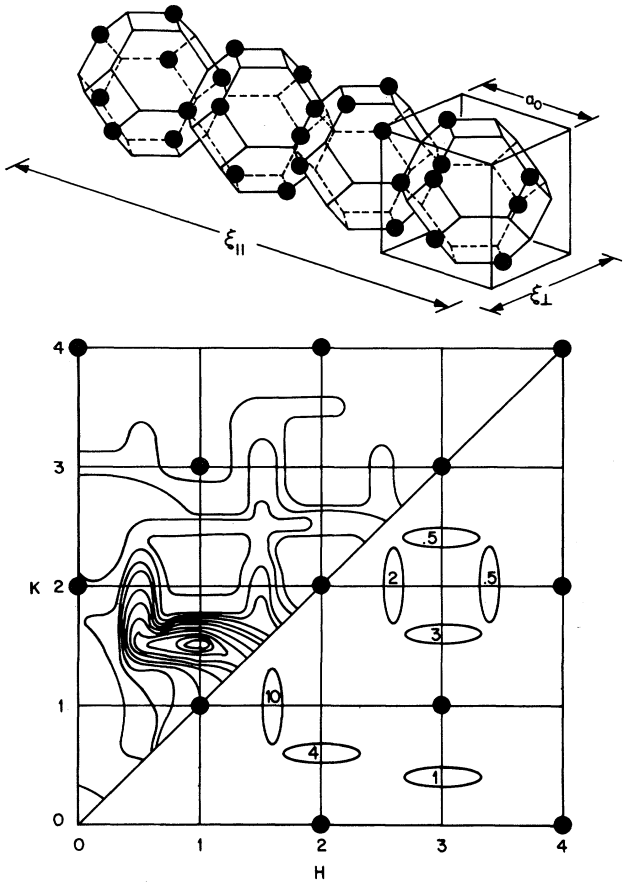

FIG. 3. Idealized model for the microdomains of ordered Ag ions on the cubo-octahedra of tetrahedral sites in β-Ag_2S. At the bottom, the calculated intensity of the diffuse scattering for this model is compared with a schematic representation of the observed diffuse scattering in the $(hk0)$ plane. The calculated intensity is above the $h=k$ mirror plane, and the observed intensity below. The observed intensities are height above background, normalized to the intensity of the disk at (1.6, 1, 0).

of the disk, $|\vec{q}_0|$, is also shown in Fig. 2, and the lattice parameter a_0 increases linearly from 4.858 Å at $T=449$ K to 4.889 Å at 568 K in agreement with earlier measurements.[6]

The structure of the correlated regions is a complicated combination of short-range order among the Ag ions and of an accompanying incommensurate displacement wave involving displacements of both the Ag and S ions from their idealized sites. A complete determination of the Ag-ion positions in terms of a set of short-range parameters is beyond the scope of the present work, and a simplified commensurate domain model is presented to illustrate the basic structural features of the Ag ions in β-Ag_2S. The average structure refinement shows that the Ag ions, although delocalized, are predominantly in the vicinity of the tetrahedral sites which form the vertices of a cubo-octahedron. The measured correlation lengths near the phase transition correspond to correlated regions consisting of a string of ~4 connected cubo-octahedra as shown in Fig. 3. We assume that nearest-neighbor Ag ions are excluded by size considerations (their separation is less than twice the tetrahedral radius of Ag^{1+}), and that there are eight silver ions per cubo-octahedron in accordance with the requirements of stoichiometry. The diffuse scattering at $\vec{Q}=h\vec{a}^*+k\vec{b}^*+l\vec{c}^*$ (where h, k, and l are continuous variables) from a domain consisting of four connected cubo-octahedra is given by $I(hkl)=P[F(hkl)-F_R(hkl)]^2$, where P is the standard polarization factor, F is the structure factor of the domain, and F_R is the structure factor for random occupancy of all 84 tetrahedral sites in the domain. The structure factors are of the form

$$F(hkl)=\sum_n p_n F_R \exp[2\pi i(hx_n+ky_n+lz_n)],$$

where x_n, y_n, and z_n are the coordinates of the site R, and p_n is 0 or 1 for the domain depending on whether a site is empty or occupied, and is $\frac{1}{3}$ for all sites for random occupancy. The F_R includes Debye-Waller factors for Ag from Ref. 6 to account for thermal motion (based on $\frac{2}{3}$ of the observed mean-square displacements, which in the average structure include displacive as well as thermal disorder), and $I(hkl)$ is suitably averaged to include all possible orientations of the domains. A number of models were considered, and the calculated intensity of the diffuse scattering for the best model, which is shown in the top of Fig. 3, is compared with the observed intensity in the bottom of Fig. 3. (There is a mirror plane along the diagonal.) The observed intensities are the peak intensity minus the background obtained from scans through the disk along the appropriate $\tilde{q}_0$, and the ellipses shown in the bottom of Fig. 3 correspond to the full width at half maximum at $T = 480$ K. Only models in which half of the Ag ions have a nearest-neighbor Ag ion at the opposite corner of the square face of the cubo-octahedron give even qualitative agreement with the observed intensity, and the best model includes displacements of these neighbors along $\langle 100 \rangle$ directions such that their separation increases by about 0.5 Å. The classic caterpillar mechanism implies the occurrence of a one-dimensional string of Ag ions in Ag_2S. The present model demonstrates that a local configuration which maximizes the distance and the angle between *pairs* of occupied next-nearest-neighbor tetrahedral sites within a larger domain gives reasonable agreement with the observed diffuse scattering.

The diffusion coefficient in Ag_2S has been obtained both by tracer (D_t) and conductivity (D_σ) measurements,[3,4] and the resulting inverse Haven's ratio $1/H_R = D_\sigma/D_t$ and the average correlation length are plotted versus temperature at the top of Fig. 2. If the charge transport in Ag_2S is via an interstitialcy mechanism, then the diffuse-scattering results are related to the microscopic diffusion process by the expression for the Haven's ratio[8]:

$$\frac{1}{H_R} = \frac{D_\sigma}{D_t} = \frac{\Gamma_\sigma}{\Gamma_t}\left(\frac{r_\sigma}{r_t}\right)^2 \frac{1}{f_t},$$

where Γ_t and r_t are tracer jump frequency and jump distance, f_t is the tracer diffusion correlation factor, and Γ_σ and r_σ are the jump frequency and transport distance of the interstitialcy. f_t will be between the value for interstitialcy ($f_t = 1$) and vacancy ($f_t = 0.5$) mechanisms for diffusion on this sublattice, as $\frac{2}{3}$ of the Ag sites are vacant. In Ag_2S there are infinite strings of connected square faces of cubo-octahedra along each cubic axis, and the caterpillar mechanism assumes a correlated jump along these strings leading to a large value of r_σ along [100]. The diffuse scattering suggests that the transport distance, in a domain model, is $4a_0$, which is eight connected squares long, and that the correlated motion is not confined to a string but includes a cylinder of Ag ions as depicted in Fig. 3. Thus the correlated ion motions are more complex than a simple collinear chain. With increasing temperature H_R^{-1} decreases, and the measured correlation length decreases, indicating a decrease in r_σ. In small measuring fields there are equal numbers of microdomains pointing along each of the cubic directions, and H_R^{-1} is an average along and across the microdomains. Therefore H_R^{-1} is compared with the average correlation length in Fig. 2. A crude estimate of the ratio of the jump frequencies, Γ_σ/Γ_t, can be made from H_R^{-1} and ξ_{av}. Assuming that r_t is between about $a_0/3$ and $a_0/2$ (there are likely to be near-neighbor, second-near-neighbor, and perhaps longer jumps) leads to Γ_σ/Γ_t between 0.1 and 0.2 near the transition. For an interstitialcy process involving n atoms, the ratio should be in the range between 1 and $1/n$, depending on whether the motion of all but the first atom is essentially instantaneous or all jumps take equal time. As there are approximately 25 silver ions taking part in the interstitialcy process near the transition, the crude estimate falls between these two limits.

The diffusion, transport, and x-ray measurements provide clear evidence for strongly correlated ionic charge transport in Ag_2S. It has been tacitly assumed that the diffuse scattering is static in origin. X-ray scattering integrates over all energy transfers and cannot distinguish between static and dynamic effects. Inelastic-neutron-scattering experiments are planned to study the diffusion process directly.

We thank T. Ohachi for the crystal, R. M. Fleming, E. I. Blount, F. Reidinger, S. M. Shapiro, and B. J. Wuensch for helpful discussions, and A. L. Stevens for technical assistance.

[1] *Fast Ion Transport in Solids*, edited by P. Vashista, J. N. Mundy, and G. K. Shenoy (North-Holland, New York, 1979).

[2]I. Yokota, J. Phys. Soc. Jpn. 21, 420 (1966).
[3]H. Okazaki, J. Phys. Soc. Jpn. 23, 355 (1967).
[4]I. Bartkowicz and S. Mrowec, Phys. Status Solidi (b) 49, 101 (1972).
[5]R. Sadanaga and S. Sueno, Mineral. J. 5, 124 (1967).
[6]R. J. Cava, F. Reidinger, and B. J. Wuensch, J. Solid State Chem. 31, 69 (1980).
[7]T. Ohachi and B. R. Pamplin, J. Cryst. Growth 42, 592 (1977).
[8]A. D. Leclaire, in *Fast Ion Transport in Solids*, edited by W. Van Gool (American Elsevier, New York, 1973), p. 51.

Undamped Second-Sound Waves in a ^{3}He-^{4}He Mixture Heated from Below

V. Steinberg[a]
Department of Physics and Astronomy, Tel Aviv University, Ramat Aviv, Israel
(Received 25 June 1980)

By using a thermodynamic analysis, it is shown that a horizontal layer of the ^{3}He-^{4}He superfluid mixture heated from below is unstable with respect to oscillatory convection. The neutral oscillations of this overstability are undamped standing second-sound waves. Estimates show the possibility to observe the predicted effect experimentally in the vicinity of the tricritical point of the ^{3}He-^{4}He mixture.

PACS numbers: 67.60.-g, 67.40.Pm

Perturbations of a noncompressible superfluid ^{3}He-^{4}He mixture lead to the appearance of second-sound waves which decay rapidly. The situation, however, changes if the system is heated from below. As shown in this note, the second-sound wave becomes an undamped standing wave. This wave is a neutral oscillation of the convective overstability.

A ^{3}He-^{4}He superfluid mixture is an interesting object for the study of the convective instability because of the high attainable temperature resolution and the low heat transport.[1] Moreover, the thermodynamic and kinetic properties of this mixture vary by several orders of magnitude within the ^{3}He-^{4}He phase diagram between the λ line and the coexistence curve.

An analysis of stationary and oscillatory instabilities in the ^{3}He-^{4}He superfluid mixture by the standard methods will be published elsewhere.[2,3] Here, we discuss only one branch of the convective instability in this system which is, in fact, the undamped second-sound wave. It is well known that in the ^{3}He-^{4}He superfluid mixture in contrast to pure He II a temperature gradient can exist in equilibrium. This temperature gradient leads to a corresponding concentration gradient, so that the superfluid ^{4}He component moves to the warm boundary and, therefore, the light ^{3}He atoms are concentrated near the cold boundary. This unusual distribution of concentration with height is a result of the superfluidity. A similar concentration distribution occurs in binary mixtures with a large abnormal thermodiffusional (Soret) effect, $k_T > 0$.[4] Such systems are unstable with respect to stationary convection when they are heated from above and with respect to oscillatory convection when heated from below.[5,6] The oscillatory instability, in this case, appears as a result of an interaction between the diffusion and thermal modes. The physical nature of the oscillatory instability in the ^{3}He-^{4}He superfluid mixture is absolutely different. Here the oscillatory instability manifests itself as a second-sound wave mode. For this mode to be undamped, the rate of supply of energy by the buoyancy force has to balance the rate of wave dissipation. This qualitative statement can be formulated in a quantitative form by using Chandrasekhar's thermodynamic principle.[7]

For the sake of simplicity, we consider a horizontal layer with free boundaries a distance l apart. Following the usual linear stability analysis, we linearize the two-fluid hydrodynamic equations for the superfluid mixture.[8] We express the small perturbations of the vertical component of the normal velocity, V_{nz}', the entropy per one gram of ^{3}He, σ', and the chemical potential of the ^{4}He atoms, μ_4', in the form

$$[V_{nz}';\sigma';\mu_4'] = (V,\sigma,\xi)e^{i\vec{k}\cdot\vec{r}}\cos(\pi z). \quad (1)$$

The dependence on coordinates in Eq. (1) is chosen in accordance with accepted free boundary conditions.

The linearized convection equations can be

